JBC Papers in Press. Published on May 8, 2007 as Manuscript M701890200
The latest version is at http://www.jbc.org/cgi/doi/10.1074/jbc.M701890200

CONTROL OF T CELL MEDIATED AUTOIMMUNITY BY METABOLITE FLUX TO N-GLYCAN BIOSYNTHESIS*

Ani Grigorian[≠1], Sung-Uk Lee[≠1], Wenqiang Tian[§], I-Ju Chen[≠], Guoyan Gao[§], Richard Mendelsohn[¶], James W. Dennis[¶,‖] and Michael Demetriou[§,≠]

From the [§]Department of Neurology and [≠]Department of Microbiology and Molecular Genetics, University of California, Irvine, CA, USA, the [¶]Samuel Lunenfeld Research Institute, Mount Sinai Hospital, 600 University Ave. Toronto, ON, Canada, M5G1X5, and the [‖]Department of Medical Genetics and Microbiology, University of Toronto, ON, Canada

Running Title: Metabolic Control of T cell Mediated Autoimmunity

Address correspondence to: Michael Demetriou, Departments of Neurology and Microbiology & Molecular Genetics, University of California, 250 Sprague Hall, Irvine, CA 92697, Tel. 949 824-9775; Fax. 949 824-9847; E-mail: mdemetri@uci.edu

Autoimmunity is a complex trait disease, where the environment influences susceptibility to disease by unclear mechanisms. T cell receptor (TCR) clustering and signaling at the immune synapse, T cell proliferation, CTLA-4 endocytosis, T_H1 differentiation and autoimmunity are negatively regulated by β1,6GlcNAc-branched N-glycans attached to cell surface glycoproteins. β1,6GlcNAc-branched N-glycan expression in T cells is dependent on metabolite supply to UDP-GlcNAc biosynthesis (hexosamine pathway) and in turn to Golgi N-acetylglucosaminyltransferases Mgat1, 2, 4 and 5. In Jurkat T cells, β1,6GlcNAc-branching in N-glycans is stimulated by metabolites supplying the hexosamine pathway including glucose, GlcNAc, acetoacetate, glutamine, ammonia or uridine, but not by control metabolites mannosamine, galactose, mannose, succinate or pyruvate. Hexosamine supplementation *in vitro* and *in vivo* also increases β1,6GlcNAc-branched N-glycans in naïve mouse T cells and suppresses TCR signaling, T cell proliferation, CTLA-4 endocytosis, T_H1 differentiation, Experimental Autoimmune Encephalomyelitis (EAE) and autoimmune diabetes in Non-Obese Diabetic (NOD) mice. Our results indicate metabolite flux through the hexosamine and N-glycan pathways conditionally regulates autoimmunity by modulating multiple T cell functionalities downstream of β1,6GlcNAc-branched N-glycans. This suggests metabolic therapy as a potential treatment for autoimmune disease.

Complex trait diseases such as autoimmunity are determined by poorly understood genetic and environmental interactions. The T cell mediated autoimmune diseases Multiple Sclerosis (MS) and Type 1 diabetes (T1D) exemplify this problem, where identical twins of Northern European descent are discordant ~60-70% of the time despite displaying an ~150-300 times higher risk than the general population prevalence of ~0.1% and ~0.4%, respectively (1;2). Genetic – environmental interactions have been established between disease-associated MHC haplotypes and specific pathogen peptides that mimic disease self antigens (3;4). The prevalence of MS and T1D change along north - south gradients, implicating ultra-violet light exposure and production of Vitamin D3 in the skin (5-7), a hormone known to negatively regulate T cell function, the MS animal model Experimental Autoimmune Encephalomyelitis (EAE) and spontaneous autoimmune diabetes in the Non-Obese Diabetic (NOD) mouse (5;8-11). However, molecular mechanisms for genetic - environmental interactions are poorly understood.

Salvage of glucosamine by the hexosamine pathway to UDP-GlcNAc is reported to suppress T cell function and EAE in mice by an unknown mechanism (12;13). *De novo* biosynthesis of UDP-GlcNAc by the hexosamine pathway utilizes glucose, acetyl-CoA, glutamine and UTP (Fig. 1), key allosteric regulators of basic metabolism, suggesting regulation of UDP-GlcNAc supply is integrated with down-stream pathways requiring this sugar-nucleotide. In this regard, the Golgi pathway to β1,6GlcNAc-branched N-glycans is

sensitive to cellular UDP-GlcNAc levels (14), and play a role in T cell function (15). Mice deficient in Golgi UDP-GlcNAc:β1,6N-acetylglucosaminyltransferase V (Mgat5) display enhanced delayed-type hypersensitivity, spontaneous kidney autoimmunity after 1 year of age, and increased susceptibility to EAE (15).

Most transmembrane receptors on mammalian cells are modified by N-glycosylation *en route* to the cell surface. The N-acetylglucosaminyltransferases I, II, IV and V, encoded by the genes Mgat1, 2, 4a/b and Mgat5, act sequentially to transfer N-acetyl-D-glucosamine (GlcNAc) from UDP-GlcNAc to N-glycan intermediates in the medial Golgi, producing mono, bi-, tri- and tetra-antennary N-glycans, respectively (16;17) (Fig. 1). (Fig. 1). Branching, and particularly the β1,6GlcNAc-branched tetra-antennary N-glycans are sub-saturating, as Mgat1, 2, 4 and 5 display decreasing affinities for UDP-GlcNAc, and enzyme concentrations also decline across the pathway (Fig. 1) (17). Galectins, a family of N-acetyllactosamine-binding animal lectins, bind cell surface glycoproteins and form a molecular lattice that negatively regulates lateral movement and endocytic loss of surface receptors and transporters (15;18-21). Galectins bind to N-glycans on surface glycoproteins with affinities proportional to GlcNAc-branching (Fig. 1) (15;18;19). β1,6GlcNAc-branched N-glycans are preferentially extended by poly-N-acetyllactosamine (ie $(Galβ1,4GlcNAcβ1,3-)_n$), further increasing avidity for galectins. However, increasing the proportion of tri-antennary structures in Mgat5 deficient cells is sufficient to rescue defects in galectin binding and surface retention of receptors (22). In addition, the number of N-glycans, an encoded feature of protein sequence (N-X-S/T), contributes to galectin avidity and regulates surface residency of receptors in a selective manner (22). With increasing hexosamine flux of UDP-GlcNAc through the Golgi to N-glycan GlcNAc branching, surface galectin binding and retention of glycoproteins with high N-glycan multiplicity (EGFR, IGFR, PDGFR, bFGFR) are enhanced before those with lower multiplicity (TGF-β receptor, CTLA-4 and GLUT-4) (22). This provides a mechanism for metabolic regulation of cellular transitions between growth (ie EGFR, IGFR, PDGFR, bFGFR) and arrest signaling (ie TGF-β receptor, CTLA-4 and GLUT-4) (22).

β1,6GlcNAc-branched N-glycans attached to the T cell receptor enhance binding to galectin-3, limiting TCR clustering at the immune synapse and increasing agonist thresholds for TCR signaling (15;22;23). After TCR activation, endocytosis rates are increased and Src-family kinases and PI3K/Erk stimulate hexosamine flux and Golgi processing to β1,6GlcNAc-branched N-glycans, thereby enhancing surface retention of the growth suppressor CTLA-4 (22). Therefore, β1,6GlcNAc-branched N-glycans regulate different receptors and at two distinct phases of the T cell response, both serving to suppress T cell activation and autoimmune mechanisms. Here we demonstrate that surface β1,6GlcNAc-branched N-glycans on T cells are regulated by the nutrient environment and metabolite supply to the hexosamine pathway. Hexosamine supplements suppress TCR sensitivity, T_H1 differentiation and autoimmunity by increasing N-glycan GlcNAc-branching in T cells. Our results indicate that genetic and environmental contributions to metabolic homeostasis and Golgi processing regulate N-glycan branching, T cell function and autoimmunity and suggest new avenues for prevention and treatment of autoimmune disease (Fig. 7).

EXPERIMENTAL PROCEDURES

FACS analysis and In Vitro proliferation assays - PL/J mice were congenic at backcross six from our original 129/Sv $Mgat5^{-/-}$ mice (24). NOD mice were obtained from Jackson laboratories at 5 weeks of age. Procedures and protocols with mice were approved by the Institutional Animal Care and Use Committee of the University of California, Irvine. Mouse cells were stained with anti-CD4 (RM4-5), anti-CD8 (53-6.7), anti-CTLA-4 (UC10-4B9), anti-CD28 (37.51) and anti-CD69 (H1.2F3), from eBioscience, *Phaseolus vulgaris* leukoagglutinating lectin (L-PHA, 4 μg/ml), *Lycopersicon esculentum* agglutinating lectin (LEA, 20 μg/ml) and 7-Aminoactinomycin D (7-AAD; 1 μg/ml) from Sigma. Purified $CD3^+$ T-cells (R&D Systems) were labeled with 5 μM 5,6-carboxyfluorescein diacetate succinimidyl ester (CFSE; Molecular Probes) in PBS for 8 min at

room temperature and stimulated with plate bound anti-CD3ε (2C11, eBioscience) in the presence or absence of GlcNAc and/or swainsonine (SW) (Sigma). Jurkat T cells were cultured in either glutamine-free RPMI 1640, 10% FBS, 10mM /20mM glucose or glucose/glutamine-free DMEM base media supplemented with 10% FBS, 1.5mM glucose. The indicated monosaccharides and/or metabolites were added daily except glucose which was added only at time zero and were titrated until a plateau was reached in L-PHA staining or toxicity was observed. The plateau or highest non-toxic dose is shown.

TCR signaling - $1x10^6$ purified splenic $CD3^+$ T-cells from $Mgat5^{+/+}$, $Mgat5^{+/-}$ and $Mgat5^{-/-}$ mice or from purified T-cell cultures incubated in the presence or absence of GlcNAc (80 mM) and/or swainsonine (0.25 μM) for 72 h were mixed with $5x10^6$ polystyrene beads (6 micron, Polysciences) coated at 4°C overnight with 0.5 μg/ml anti-CD3ε antibody (2C11, eBioscience) and pelleted at 5,000 rpm for 15 s, incubated at 37˚C for the indicated times, and then solubilized with ice-cold 50 mM Tris pH 7.2, 300 mM NaCl, 1.0% Triton X-100, protease inhibitor cocktail (Boehringer Mannheim) and 2 mM Orthovanadate for 20 min. Cell lysates were separated on Nupage10 % BIS-TRIS gels (Invitrogen) under reducing conditions, transferred to polyvinylidene difluoride membranes and immunoblotted with rabbit anti-phospho-Zap70 Ab (CST), rabbit anti-phospho-LAT Ab (Upstate), and/or anti-actin Ab (Santa Cruz).

MS/MS mass spectroscopy - For MS/MS mass spectroscopy to determine sugar nucleotide levels, Jurkat T-cell pellets (20x106 cells) were resuspended in cold 300 ml methanol:water (1:1) solution containing maltose as an internal standard, vortexed for 10 seconds, and then pipetted into tubes containing 600 ml of chloroform:methanol (C:M) (3:2). Maltose (100 pmoles) was added to each sample as internal standard. Samples were vortexed for 1 minute, and then centrifuged at 14,000 rpm for 5 minutes at 4°C. Supernatants were collected, and an equal volume of C:M (1:1) was added, followed by a second extraction. The pooled aqueous fraction containing the hydrophilic metabolite was dried with a speedvac, passed over C18 SepPak in water, dried and stored at -80°C. Prior to injection, the samples were dissolved in 100 ml methanol:water (1:1). The samples were injected at 150 ml/hr, and analyzed on a 4000QTRAP (Mass Spectrometer (SCIEX). The metabolites were identified by their transitions in MS/MS, and quantified using the Analyst Software (Applied Biosystems- SCIEX), which measured the area under the curve for major fragment ion (M2) corresponding to each parent ion (M1). Collision energy (CE), declustering potential (DP) and ion spray voltage (IS) were optimized for each metabolite. UDP-GlcNAc (M1= 605.9, and M2 = 385.0 with setting DP, -40; CE, -38; and IS, -3500) and UDP-Gal (M1= 564.9, and M2 = 323.0 with setting DP, +80; CE, +23; IS, +5500) were measured in negative and positive, respectively. Maltose was measured in negative mode (M1= 341, and M2 = 161 with setting DP, -40; CE, -13; and IS, -4000). Standards for maltose, UDP-GlcNAc and UDP-Gal showed sensitivity to 15 pmoles and linearity to 10 nmoles. Data is reported as UDP-HexNAc and UDP-Hex due to potential inter-conversion of UDP-GlcNAc to UDP-GalNAc and UDP-Gal to UDP-Glc by 4'-epimerase activity, sugar nucleotides not distinguished in M1.

In Vivo GlcNAc Treatment - GlcNAc was administered orally in age and sex-matched PL/J littermate mice by adding GlcNAc to their drinking water at various concentrations. Fresh GlcNAc was given daily for 5 days, with amount consumed approximated by determining the volume remaining after 24h. After 5 days of treatment, harvested splenocytes were stained and analyzed by FACS.

Cytokine ELISA - Supernatant from splenocyte and/or T cell cultures stimulated with MBP and/or anti-CD3ε (2C11, eBioscience) in the presence or absence of GlcNAc and/or SW were tested for IFN-γ, IL-6, and/or IL-4 levels by ELISA. Microtiter plates were coated with 50 μl of anti-IFN-γ (1 μg/ml, clone AN-18; eBioscience), anti-IL-6 (1.5 μg/ml, clone MP5-20F3; eBioscience), or anti-IL-4 (2 μg/ml, clone 11B11; eBioscience) overnight at 4°C. Supernatants were applied at 50 μl/well and incubated for 2 h at room temperature. Captured cytokines were detected using biotinylated anti-IFN-γ (1 μg/ml, clone R4-6A2; eBioscience), anti-IL-6 (1 μg/ml, clone MP5-32C11; eBioscience) or anti-IL-4 (1 μg/ml, clone BVD6-24G2; eBioscience) and detected using Avidin Horse Radish Peroxidase (eBioscience) at 1:500x dilution and o-Phenylenediamine

dihydrochloride OPD tablets (Sigma) according to the manufacturer's protocols. Recombinant IFN-γ, IL-6, or IL-4 (eBioscience) was used as a standard.

Adoptive transfer EAE and NOD Diabetes - Adoptive transfer EAE was induced by subcutaneous immunization of wild-type PL/J mice with 100 μg of bovine Myelin Basic Protein (MBP, Sigma) emulsified in Complete Freund's Adjuvant containing 4 mg/ml heat-inactivated *Mycobacterium tuberculosis* (H37 RA; Difco, Detroit, MI) distributed over three spots on the hind flank. Splenocytes were harvested after 11 days and stimulated *in vitro* with 50 μg/ml MBP in the presence or absence of 40 mM GlcNAc (Sigma) added daily. After 96 h incubation, $CD3^+$ T cells were purified by negative selection (R&D Systems) and injected i.p. into naïve PL/J $Mgat5^{+/-}$ recipient mice. Trypan blue exclusion determined <5% dead cells under both culture conditions. Mice were scored daily for clinical signs of EAE over the next 30 days with the observer blinded to treatment conditions. Mice were examined daily for clinical signs of EAE and scored in a blinded fashion as follows: 0, no disease; 1, loss of tail tone; 2, hindlimb weakness; 3, hindlimb paralysis; 4, forelimb weakness or paralysis and hindlimb paralysis; 5, moribund or dead. GlcNAc was administered orally to female NOD mice by adding fresh GlcNAc at a concentration of 250*ug*/ml to the drinking water every 3 days. Spontaneous diabetes in wildtype NOD mice was diagnosed following two consecutive positive tests for glycosuria of ≥2000 mg/dl by Chemstrip (Accu-chek, Roche) 1 week apart.

RESULTS

T cell thresholds and fractional changes in β1,6GlcNAc-branching - Conditional or metabolic regulation of T cell activation thresholds could be expected to be sensitive to small incremental changes in N-glycan branching. To test this hypothesis, we compared the agonist sensitivity of primary T cells from $Mgat5^{+/+}$, $Mgat5^{+/-}$ and $Mgat5^{-/-}$ mice. $Mgat5^{+/-}$ T cells show a ~20-25% reduction in β1,6GlcNAc-branched N-glycans relative to $Mgat5^{+/+}$ cells as indicated by L-PHA (*Phaseolus Vulgaris* Leukoagglutinin) binding, a plant lectin specific for these structures (Fig. 2*A*)(15;23). Stimulation of purified $CD3^+$ T cells with anti-CD3- coated microbeads demonstrates that $Mgat5^{+/-}$ cells are intermediate compared to $Mgat5^{+/+}$ and $Mgat5^{-/-}$ cells for TCR signaling as shown by enhanced phosphorylation of Zap-70 and LAT (Fig. 2*B*). $Mgat5^{+/-}$ T cells are similarly intermediate for TCR-mediated proliferation, as shown by tracking cell division with CFSE (Fig. 2*C*). To confirm that small reductions in β1,6GlcNAc-branched N-glycans enhance TCR sensitivity, we treated wild type cells with minimal concentrations of swainsonine (SW). SW is a specific inhibitor of mannosidase II that blocks GlcNAc branching in N-glycans, and is known to enhance T cell proliferation and T_H1 differentiation (23;25). At low levels of anti-CD3 stimulation, partial reductions in β1,6GlcNAc-branched N-glycans by low doses of swainsonine significantly enhance wild type T cell proliferation (Fig. 2*D*) (25;26). Thus, changes in T cell activation thresholds can be readily detected with as little as ~20-25% variations in β1,6GlcNAc-branched N-glycans.

Metabolic flux through the hexosamine pathway regulates β1,6GlcNAc-branched N-glycans in T cells - The expression of tri-(ie β1,4) and tetra-(ie β1,6) antennary GlcNAc-branched N-glycans in cultured cells is sensitive to changes in the intracellular concentration of UDP-GlcNAc (14;22), which enters the Golgi via UDP-GlcNAc transporters (27). The addition of GlcNAc to cultured cells supplements UDP-GlcNAc pools following uptake by bulk endocytosis, 6-phosphorylation and conversion to UDP-GlcNAc (Fig. 1) (14;22). Glucose, glutamine, acetyl-CoA and UTP are metabolites required by the hexosamine pathway for *de novo* UDP-GlcNAc biosynthesis (Fig. 1). TCR activation of mouse T cells increases Mgat5 gene expression (15), glucose uptake (28), UDP-HexNAc levels (22) and β1,6GlcNAc-branched N-glycans (23). GlcNAc supplementation of activated T cells further enhances UDP-HexNAc levels, increasing the UDP-HexNAc:UDP-Hex ratio upto ~6 fold (22). To determine whether hexosmaine metabolite supplementation enhances expression of cell surface galectin ligands (ie N-glycan GlcNAc-branching and poly-N-acetyllactosamine) in resting T cells, cells were titrated with various metabolites until a plateau was reached in L-PHA staining or toxicity was observed. Surface levels of β1,6GlcNAc-branched N-glycans (ie L-PHA

staining) and poly-N-acetyllactosamine (indicated by staining with the plant lectin *Lycopersicon esculentum* agglutinin (LEA)) on non-TCR activated human Jurkat T-cells were increased by supplementing the hexosamine pathway with high glucose, GlcNAc, acetoacetate, glutamine, ammonia or uridine but not with control metabolites mannosamine, galactose, mannose, succinate or pyruvate (Fig. 3, *A* and *B*; supplemental Fig. 1, *A* and *B*). Supplementing resting mouse *ex vivo* splenocytes with GlcNAc, glucose or uridine *in vitro* significantly raised β1,6GlcNAc-branched N-glycans in $CD4^+$ T cells (Fig. 4*A*). In non-T cells, GlcNAc supplementation also increases tri-antennary structures (22) and these are likely also enhanced in supplemented T cells. MS/MS mass spectroscopy confirmed that GlcNAc, Glucose, and uridine supplements raised intracellular UDP-HexNAc levels in non-TCR activated Jurkat T cells (Fig. 3*C*). On a per cell basis, UDP-HexNAc levels in Jurkat T cells appear lower than that reported for CHO cells (29); however T cells are smaller and have a markedly higher nuclear to cytoplasmic ratio, making direct comparisons difficult. Co-supplementation of GlcNAc and uridine in resting Jurkat and wildtype mouse T cells were additive and more effective than doubling the GlcNAc concentration (Fig. 3*D*; Fig. 4*B*). Supplementing the drinking water of $Mgat5^{+/-}$ or $Mgat5^{+/+}$ mice with GlcNAc increased β1,6GlcNAc-branched N-glycans up to ~40% on $CD4^+$ T cells *in vivo* (Fig. 4*C*; supplemental Fig. 2*A*). Taken together, these data indicate that production of high affinity galectin ligands (eg. β1,6GlcNAc-branched N-glycans and poly-N-acetyllactosamine) are limited in T cells by the availability of key intermediates of glucose, lipid, nitrogen and nucleotide metabolism.

Suppression of T cell function and autoimmunity by the hexosamine pathway is dependent on N-glycan GlcNAc-branching - Genetically induced reductions in T cell β1,6GlcNAc-branching weaken the galectin lattice, enhancing agonist induced TCR clustering and signaling, T_H1 differentiation (ie increased IFNγ and reduced IL-4 production), CTLA-4 endocytosis, T cell proliferation and susceptibility to autoimmunity (Fig. 2, *A-C* and (15;22;23)). Consequently, metabolic enhancement of N-glycan GlcNAc branching, particularly β1,6GlcNAc-branching, should strengthen the galectin lattice and negatively regulate these phenotypes. Hexosamine supplementation of wild-type resting T cells with GlcNAc inhibited anti-CD3 induced phosphorylation of lck at activating Y^{394} and Zap-70 (Fig. 5*A*). TCR signal strength regulates expression of the T cell activation marker CD69 as well as production of IFNγ relative to IL-4 (30), and as expected, both are inhibited by hexosamine supplementation (Fig. 5, *B* and *C,* supplemental Fig. 3, *A-C*). CTLA-4 retention at the surface of blasting T cells is promoted by TCR signaling mediated increases in hexosamine flux and Golgi processing to β1,6GlcNAc-branched N-glycans (22). GlcNAc supplementation significantly increases surface levels of CTLA-4 relative to CD28 in T cell blasts (Fig. 5*D*), receptors that compete for binding to CD80/86 on antigen presenting cells to negatively and positively regulate growth arrest, respectively (31). Tracking cell division of purified T cells using CFSE labeling demonstrates that hexosamine supplementation inhibits T cell proliferation without inducing cellular toxicity as measured by 7-AAD (Fig. 5*E*; supplemental Fig. 3, *D-F*). Very importantly, all observed effects of hexosamine supplementation on T cell function are dependent on N-glycans, as they could be reversed by blocking N-glycan GlcNAc branching beyond mono-antennary with SW and/or the mannosidase I inhibitor deoxymannojirimycin (DMN, Fig. 1) (Figs. 5 *A-E*; supplemental Fig. 2*B*; supplemental Fig. 3, *B, C, E,* and *F*). These data demonstrate that hexosamine supplementation controls three temporally distinct autoimmune regulatory phenotypes, namely T cell activation thresholds, T_H1 differentiation and CTLA-4 endocytosis, by enhancing GlcNAc branching in N-glycans.

Next, we determined whether hexosamine induced changes in GlcNAc-branched N-glycans suppresses T cell mediated autoimmunity. The MS model EAE may be induced by adoptive transfer of myelin antigen specific T cells into naïve mice, leading to inflammatory demyelination of axons and progressive motor weakness. Splenocytes from myelin basic protein (MBP) immunized wild-type PL/J mice were re-stimulated *in vitro* with MBP in the presence or absence of GlcNAc, then transferred to naïve mice for induction of EAE. Re-stimulation in the presence of GlcNAc increased β1,6GlcNAc-branched N-glycans and

poly-N-acetyllactosamine expression and inhibited production of the T_H1 cytokine IFN-γ while promoting secretion of the T_H2 inducing/T_H1 inhibitory cytokine IL-6 (Fig. 6, *A* and *B*) (32). After adoptive transfer of the T cells into naïve PL/J mice, mice receiving the GlcNAc-supplemented cells showed dramatically reduced incidence and severity of EAE compared to mice given untreated cells (Fig. 6*C*).

To determine whether oral GlcNAc supplementation inhibits spontaneous autoimmunity, we supplemented the drinking water of female NOD mice at 250μg/ml, a concentration that maximally raises β1,6GlcNAc-branched N-glycans in $CD4^+$ T cells *in vivo* (Fig. 4*C*). GlcNAc supplementation starting between the 5th and 6th week of age significantly reduced development of autoimmune diabetes (Fig. 6*D*). Insulitis begins at 3-4 weeks of age in NOD mice (11), suggesting initiation of GlcNAc supplementation prior to insulitis may further reduce development of diabetes.

Others have demonstrated that *in vitro* and/or *in vivo* supplementation of mice with Glucosamine (GlcN) inhibits T cell activation, T_H1 responses as well as graft rejection and EAE; but the mechanism is unknown (12;13). GlcN enters the hexosamine pathway following 6-phosphorylation (Fig. 1). Our data demonstrates that GlcN also increases β1,6GlcNAc-branching in T cells, with maximal changes occurring at ~100-150 μM (supplemental Fig. S1*C*), the same concentration that others have found inhibit proliferation and T_H1 differentiation (13). Taken together, these data indicate key metabolites shared by hexosamine, glycolysis, lipid (free fatty acids to acetyl-CoA), amino acid (ie ammonia/glutamine) and nucleotide metabolism conditionally regulate thresholds for T cell function and autoimmunity by altering GlcNAc-branching in N-glycans.

DISCUSSION

GlcNAc-branching in N-glycans titrates binding to galectins, forming a molecular lattice at the cell surface that negatively regulates TCR sensitivity, T_H1 differentiation, CTLA-4 endocytosis, and the threshold to autoimmunity (15;22;23). Here we demonstrate that T cell function and autoimmunity are regulated by the nutrient environment and metabolite supply to the hexosamine pathway in a N-glycan GlcNAc-branching-dependent manner. This implies that genetic contributions to intracellular metabolic homeostasis, coupled with the nutrient environment, regulate GlcNAc-branching in N-glycans, and thereby autoimmune susceptibility. Autoimmunity is a complex trait disease, where genetic susceptibility is modulated by the environment via unclear mechanisms. In this regard, metabolic regulation of GlcNAc-branching provides an environmental mechanism to influence genetic predisposition to autoimmunity (Fig. 7).

GlcNAc and GlcN supplement the hexosamine pathway (Fig. 1), increase β1,6GlcNAc-branched N-glycans and inhibit T cell function and autoimmunity (Fig. 3*B*, 4*A*, 5*A-E*, 6*A-C* and supplemental Fig. S1*C*) (12;13). GlcN enters cells via glucose transporters, allowing a ~200-400 fold reduction in effective concentration relative to GlcNAc, which is taken up by bulk endocytosis. However, maximal increases in β1,6GlcNAc-branched N-glycans are ~2-4 fold greater with GlcNAc than GlcN. Moreover, increasing concentrations of GlcN (>200μM), unlike GlcNAc, reduces β1,6GlcNAc-branched N-glycans. GlcN-6-P but not GlcNAc-6-P is a potent inhibitor of glutamine-fructose-6-P aminotransferase (GFAT), the rate-limiting enzyme shunting fructose-6-phosphate into the hexosamine pathway (33). GlcN-6-P may also exit the hexosamine pathway to enter glycolysis following de-amination by glucosamine-6-phosphate deaminase (GNPD) (Fig. 1). These data suggest GlcNAc functions as a better inducer of β1,6GlcNAc-branching as GFAT product inhibition and/or enhanced GNPD activity may limit the effectiveness of GlcN. In this regard, GlcNAc is predicted to be a superior therapeutic agent for prevention and/or treatment of human autoimmunity. Indeed, 8 of 12 children with severe treatment-resistant inflammatory bowel disease had significant clinical improvement following ~2 years of treatment with 3-6g/day of oral GlcNAc (34). Assuming a weight of 40-50kg for these children, which was not reported in the study, the dose used is ~60-150mg/kg/day, similar to the 20-160mg/kg/day dose that maximally raises T cell β1,6GlcNAc branching and inhibits autoimmune diabetes in mice. No significant adverse effects were noted over ~2 yrs of treatment**,** suggesting GlcNAc therapy is likely to be a safe therapeutic approach in humans.

In addition to the N-glycan GlcNAc transferases, UDP-GlcNAc is a sugar-nucleotide donor for the Golgi O-glycan pathway (35) and cytoplasmic O-GlcNAc transferase (36). UDP-GlcNAc may also be converted to UDP-GalNAc, the sugar-nucleotide utilized by GalNAc transferases to initiate O-glycosylation at Ser/Thr residues. Our data do not exclude metabolic induced changes in these or other pathways requiring UDP-GlcNAc or UDP-GalNAc. However, the N-glycan pathway-specific inhibitor SW reverses all observed effects of GlcNAc supplementation on T-cell function (Fig. 2*D*; Fig. 5, *A-E*; supplemental Fig. 3, *B, C, E, and F*). Similarly, GlcNAc dependent inhibition of receptor endocytosis is reversed by mutation of N-glycosylation sites (ie N-X-S/T) and by knockout of Mgat1 (22). Thus, metabolic regulation of GlcNAc-branched N-glycans is necessary and sufficient to produce the observed autoimmune inhibitory T cell phenotypes (ie T cell activation thresholds, T_H1 differentiation and CTLA-4 surface expression), identifying N-glycans as a major target of hexosamine mediated inhibition of autoimmunity.

β1,6GlcNAc-branched N-glycans are present on β1 integrins and negatively regulate cell adhesion and promote tumor cell motility (19;24;37). Substratum and cell-cell adhesion regulates several aspects of T cell activation and migration. Antibodies that disrupt binding of T cell-associated $\alpha_4\beta_1$ integrin to Vascular Cell Adhesion Molecule – 1 (VCAM-1) on activated endothelium negatively regulates EAE and MS by blocking T cell recruitment to the CNS (38;39). β1,6 GlcNAc-branching in β1 integrins negatively regulates cell adhesion (24;37;40) including inhibition of T cell binding to VCAM-1 *in vitro* (M. Demetriou, unpublished data), which may limit T cell recruitment to the CNS *in vivo*. Mgat5-deficient macrophages have decreased motility and phagocytosis (19), a phenotype that may promote autoimmunity by inhibiting clearance of apoptotic cells (41).

Mutations in genes of apparently distinct pathways for TCR signal strength (42-44), T_H1 differentiation (45) and CTLA-4 expression (46) promote T cell mediated autoimmunity. However, targets of N-glycan GlcANc branching include TCR, CTLA-4 and other surface glycoproteins (15;22;23), and taken with our results, N-glycan processing appears to serve as an intermediate in the conditional regulation of the cellular immune system. The hexosamine/Golgi processing pathways regulate at least three temporally distinct T cell phenotypes (activation, T_H differentiation, arrest) (15;22;23). This suggests that the hexosamine and Golgi pathways have co-evolved with the larger regulatory network that controls the cellular immune system. With a better understanding of the hexosamine pathway and its regulation of the immune system *in vivo*, metabolic therapy of human autoimmune disease may prove to be a useful intervention (47).

REFERENCES

1. Ebers, G. C., Bulman, D. E., Sadovnick, A. D., Paty, D. W., Warren, S., Hader, W., Murray, T. J., Seland, T. P., Duquette, P., Grey, T., and . (1986) *N.Engl.J.Med.* **315,** 1638-1642

2. Redondo, M. J., Yu, L., Hawa, M., Mackenzie, T., Pyke, D. A., Eisenbarth, G. S., and Leslie, R. D. (2001) *Diabetologia* **44,** 354-362

3. Oldstone, M. B. (1987) *Cell* **50,** 819-820

4. Wucherpfennig, K. W. and Strominger, J. L. (1995) *Cell* **80,** 695-705

5. Munger, K. L., Zhang, S. M., O'Reilly, E., Hernan, M. A., Olek, M. J., Willett, W. C., and Ascherio, A. (2004) *Neurology* **62,** 60-65

6. Green, A., Gale, E. A., and Patterson, C. C. (1992) *Lancet* **339,** 905-909

7. Hypponen, E., Laara, E., Reunanen, A., Jarvelin, M. R., and Virtanen, S. M. (2001) *Lancet* **358,** 1500-1503

8. Tsoukas, C. D., Provvedini, D. M., and Manolagas, S. C. (1984) *Science* **224,** 1438-1440

9. Lemire, J. M. and Archer, D. C. (1991) *J.Clin.Invest* **87,** 1103-1107

10. Zella, J. B., McCary, L. C., and DeLuca, H. F. (2003) *Arch.Biochem.Biophys.* **417,** 77-80

11. Anderson, M. S. and Bluestone, J. A. (2005) *Annu.Rev.Immunol.* **23,** 447-485

12. Ma, L., Rudert, W. A., Harnaha, J., Wright, M., Machen, J., Lakomy, R., Qian, S., Lu, L., Robbins, P. D., Trucco, M., and Giannoukakis, N. (2002) *J.Biol.Chem.* **277,** 39343-39349

13. Zhang, G. X., Yu, S., Gran, B., and Rostami, A. (2005) *J.Immunol.* **175,** 7202-7208

14. Sasai, K., Ikeda, Y., Fujii, T., Tsuda, T., and Taniguchi, N. (2002) *Glycobiology* **12,** 119-127

15. Demetriou, M., Granovsky, M., Quaggin, S., and Dennis, J. W. (2001) *Nature* **409,** 733-739

16. Kornfeld, R. and Kornfeld, S. (1985) *Annu.Rev.Biochem.* **54,** 631-664

17. Schachter, H. (1991) *Glycobiology* **1,** 453-461

18. Brewer, C. F., Miceli, M. C., and Baum, L. G. (2002) *Curr.Opin.Struct.Biol.* **12,** 616-623

19. Partridge, E. A., Le Roy, C., Di Guglielmo, G. M., Pawling, J., Cheung, P., Granovsky, M., Nabi, I. R., Wrana, J. L., and Dennis, J. W. (2004) *Science* **306,** 120-124

20. Ohtsubo, K., Takamatsu, S., Minowa, M. T., Yoshida, A., Takeuchi, M., and Marth, J. D. (2005) *Cell* **123,** 1307-1321

21. Nieminen, J., Kuno, A., Hirabayashi, J., and Sato, S. (2007) *J.Biol.Chem.* **282,** 1374-1383

22. Lau, K. S., Partridge, E. A., Grigorian, A., Silvescu, C. I., Reinhold, V. N., Demetriou, M., and Dennis, J. W. (2007) *Cell* **129,** 123-134

23. Morgan, R., Gao, G., Pawling, J., Dennis, J. W., Demetriou, M., and Li, B. (2004) *J.Immunol.* **173,** 7200-7208

24. Granovsky, M., Fata, J., Pawling, J., Muller, W. J., Khokha, R., and Dennis, J. W. (2000) *Nat.Med.* **6,** 306-312

25. Wall, K. A., Pierce, J. D., and Elbein, A. D. (1988) *Proc.Natl.Acad.Sci.U.S.A* **85,** 5644-5648

26. Tulsiani, D. R., Harris, T. M., and Touster, O. (1982) *J.Biol.Chem.* **257,** 7936-7939

27. Hirschberg, C. B., Robbins, P. W., and Abeijon, C. (1998) *Annu.Rev.Biochem.* **67,** 49-69

28. Frauwirth, K. A. and Thompson, C. B. (2004) *J.Immunol.* **172,** 4661-4665

29. Tomiya, N., Ailor, E., Lawrence, S. M., Betenbaugh, M. J., and Lee, Y. C. (2001) *Anal.Biochem.* **293,** 129-137

30. Tao, X., Constant, S., Jorritsma, P., and Bottomly, K. (1997) *J.Immunol.* **159,** 5956-5963

31. Alegre, M. L., Frauwirth, K. A., and Thompson, C. B. (2001) *Nat.Rev.Immunol.* **1,** 220-228

32. Diehl, S. and Rincon, M. (2002) *Mol.Immunol.* **39,** 531-536

33. Broschat, K. O., Gorka, C., Page, J. D., Martin-Berger, C. L., Davies, M. S., Huang Hc, H. C., Gulve, E. A., Salsgiver, W. J., and Kasten, T. P. (2002) *J.Biol.Chem.* **277,** 14764-14770

34. Salvatore, S., Heuschkel, R., Tomlin, S., Davies, S. E., Edwards, S., Walker-Smith, J. A., French, I., and Murch, S. H. (2000) *Aliment.Pharmacol.Ther.* **14,** 1567-1579

35. Schachter, H. and Brockhausen, I. (1989) *Symp.Soc.Exp.Biol.* **43,** 1-26

36. Wells, L. and Hart, G. W. (2003) *FEBS Lett.* **546,** 154-158

37. Demetriou, M., Nabi, I. R., Coppolino, M., Dedhar, S., and Dennis, J. W. (1995) *J.Cell Biol.* **130,** 383-392

38. Yednock, T. A., Cannon, C., Fritz, L. C., Sanchez-Madrid, F., Steinman, L., and Karin, N. (1992) *Nature* **356,** 63-66

39. Polman, C. H., O'Connor, P. W., Havrdova, E., Hutchinson, M., Kappos, L., Miller, D. H., Phillips, J. T., Lublin, F. D., Giovannoni, G., Wajgt, A., Toal, M., Lynn, F., Panzara, M. A., and Sandrock, A. W. (2006) *N.Engl.J.Med.* **354,** 899-910

40. Nakagawa, H., Zheng, M., Hakomori, S., Tsukamoto, Y., Kawamura, Y., and Takahashi, N. (1996) *Eur.J.Biochem.* **237,** 76-85

41. Scott, R. S., McMahon, E. J., Pop, S. M., Reap, E. A., Caricchio, R., Cohen, P. L., Earp, H. S., and Matsushima, G. K. (2001) *Nature* **411,** 207-211

42. Bachmaier, K., Krawczyk, C., Kozieradzki, I., Kong, Y. Y., Sasaki, T., Oliveira-dos-Santos, A., Mariathasan, S., Bouchard, D., Wakeham, A., Itie, A., Le, J., Ohashi, P. S., Sarosi, I., Nishina, H., Lipkowitz, S., and Penninger, J. M. (2000) *Nature* **403,** 211-216

43. Chiang, Y. J., Kole, H. K., Brown, K., Naramura, M., Fukuhara, S., Hu, R. J., Jang, I. K., Gutkind, J. S., Shevach, E., and Gu, H. (2000) *Nature* **403,** 216-220

44. Krawczyk, C., Bachmaier, K., Sasaki, T., Jones, R. G., Snapper, S. B., Bouchard, D., Kozieradzki, I., Ohashi, P. S., Alt, F. W., and Penninger, J. M. (2000) *Immunity.* **13,** 463-473

45. Bettelli, E., Sullivan, B., Szabo, S. J., Sobel, R. A., Glimcher, L. H., and Kuchroo, V. K. (2004) *J.Exp.Med.* **200,** 79-87

46. Waterhouse, P., Penninger, J. M., Timms, E., Wakeham, A., Shahinian, A., Lee, K. P., Thompson, C. B., Griesser, H., and Mak, T. W. (1995) *Science* **270,** 985-988

47. Niehues, R., Hasilik, M., Alton, G., Korner, C., Schiebe-Sukumar, M., Koch, H. G., Zimmer, K. P., Wu, R., Harms, E., Reiter, K., von Figura, K., Freeze, H. H., Harms, H. K., and Marquardt, T. (1998) *J.Clin.Invest* **101,** 1414-1420

FOOTNOTES

1 These authors contributed equally to this work.

*This research was supported by grants from Canadian Institutes for Health Research to JWD and from the National Multiple Sclerosis Society, the Juvenile Diabetes Research Foundation, the Wadsworth Foundation and the US National Institute of Allergy and Infectious Disease, National Institutes of Health to M.D.

The authors declare that they have no competing financial interests.

FIGURE LEGENDS

Fig. 1. Regulation of GlcNAc-branched N-glycan biosynthesis by the Hexosamine and N-glycan pathways**.** UDP-GlcNAc is required by the N-acetylglucosaminyltransferases Mgat1, 2, 3, 4 & 5 and iGnT. Size of the arrows for Mgat1, 2, 4 and 5 depicts relative affinity for UDP-GlcNAc, with K_m below arrows. Cytosolic UDP-GlcNAc enters the Golgi via anti-porter exchange with Golgi UMP, a reaction product of the N-acetylglucosaminyltransferases. Galectins bind N-acetyllactosamine, with avidity increasing in proportion to the number N-acetyllactosamine units (ie GlcNAc branching). β1,6GlcNAc-branching by Mgat5 promotes poly-N-acetyllactosamine production, further enhancing avidity for galectins. DMN, deoxymannojirimycin; SW, swainsonine; GI, glucosidase I; GII, glucosidase II; MI, mannosidase I; MIIx, mannosidase IIx; GalT3, galactosyltransferase3. A bypass pathway involving Mgat1 activity prior to mannosidase II is not shown.

Fig. 2. β1,6GlcNAc-branched N-glycan expression and dose-dependent regulation of T cell function. *A*, L-PHA (*Phaseolus Vulgaris* Leukoagglutinin) FACS analysis of $CD4^+$ T cells from the indicated genotypes. Background fluorescence in L-PHA stained $Mgat5^{-/-}$ $CD4^+$ T cells is the same as non-L-PHA stained $Mgat5^{+/+}$ $CD4^+$ T cells, confirming previous observations that L-PHA specifically binds β1,6GlcNAc-branched N-glycans (15). *B*, Purified $CD3^+$ T-cells of the indicated genotypes were incubated at 37°C with anti-CD3 antibody-coated microbeads for various times, lysed and western blotted (WB). *C*, Purified $CD3^+$ T-cells were labeled with CFSE, stimulated for 3 days and analyzed by FACS.

Shown are gated on $CD4^+$ cells. *D*, Purified $CD3^+$ T-cells were labeled with CFSE (lower panel) or left unstained (upper panel), stimulated for 5 days in the presence or absence of SW, and analyzed by FACS. Shown is L-PHA MFI (upper panel) and percentage increase in the number of proliferating $CD4^+$ T cells relative to cells stimulated with 62.5ng/ml anti-CD3 (lower panel). All data are gated on $CD4^+$ cells. The results are representative of at least three independent experiments.

Fig. 3. Metabolite supply to the hexosamine pathway regulates β1,6GlcNAc-branched N-glycan expression in Jurkat T-cells. *A-D*, The indicated monosaccharides and metabolites were cultured with Jurkat T-cells for 3 days, stained with L-PHA-FITC in triplicate and analyzed by FACS *(A,B,D)* or lysed and analyzed by MS/MS mass spectroscopy for sugar-nucleotide expression *(C)*. Green, blue and red lines in *(B)* refer to altered glucose concentration in the culture media as indicated; all others were cultured in 10 mM glucose. UDP-HexNAc and UDP-Hex levels in non-supplemented cells were below the detection level of our assay. Detection via HPLC indicates GlcNAc supplementation increases the UDP-HexNAc:UDP-Hex ratio upto ~6 fold in TCR activated mouse T cells (22). Error bars are present in *(A,B,D)* and represent mean ± standard error of triplicate staining. P values in *D* are by ANOVA and the Newman-Keuls multiple comparison test with non-supplemented cells or as indicated. *p<0.05, **p<0.01, ***p<0.001

Fig. 4. Metabolite supply to the hexosamine pathway regulates β1,6GlcNAc-branched N-glycan expression in resting primary mouse T-cells. *A and B*, The indicated monosaccharides and metabolites were cultured with unstimulated mouse splenocytes for 3 days, stained with L-PHA-FITC in triplicate and analyzed by FACS. The results are representative of at least three independent experiments. Error bars are present in all panels and represent mean ± standard error of triplicate samples. *C*, Splenocytes from $Mgat5^{+/-}$ mice orally supplemented with GlcNAc for 5 days via their drinking water at the indicated concentrations were stained with L-PHA-FITC in triplicate and analyzed by FACS. On average, mice drank ~4.6 ± 0.25 ml/day, estimated by determining the amount of GlcNAc solution remaining daily. For a 28.5g mouse, the approximate mg/kg doses received is 10, 20, 40, 80 and 160 respectively. Data shown are an average from two independent experiments, each with triplicate staining. n = number of mice. Error bars are mean ± standard error. P values in *B and C* are by ANOVA and the Newman-Keuls multiple comparison test with non-supplemented cells/mice or as indicated. *p<0.05, **p<0.01, ***p<0.001

Fig. 5. Regulation of T-cell function by the hexosamine pathway**.** *A*, Resting purified $CD3^+$ T-cells from wild-type mice pre-incubated for 2 days in the absence or presence of 80mM GlcNAc and/or 250ηM swainsonine (SW) as indicated were stained with L-PHA-FITC in triplicate or incubated at 37°C with anti-CD3 antibody-coated microbeads for various times, lysed and western blotted (WB). Bands quantified using Gel Pro Analyzer software were first normalized to the resting vehicle treated lane and then to actin. Numbers are shown below each band. Note that phosphorylation of lck Y^{394} is reduced at 3 and 10 min relative to rest in GlcNAc treated but not vehicle and GlcNAc+SW treated cells. *B-D*, Wild-type $CD3^+$ T-cells were stimulated with anti-CD3 antibody in the presence or absence of GlcNAc, swainsonine (SW) and/or deoxymannojirimycin (DMN) as indicated for 2 days *(C),* 3 days *(B)*, or 4 days *(D)*. *B*, Cells were analyzed by FACS for CD69 staining. The results are representative of three independent experiments. Error bars are present in all panels and represent mean ± standard error of triplicate samples. Anti-CD3 = 62.5ηg/ml, SW = 250ηM, DMN = 2mM. *C*, Harvested supernatant from triplicate wells were analyzed by ELISA for IFNγ and IL-4 and shown as a ratio of IFNγ to IL-4, eliminating effects of GlcNAc and/or swainsonine on T cell number. Similar data for IFNγ was obtained at 3 days using splenocytes (see supplemental Fig. 3*C*). Anti-CD3 = 62.5ηg/ml, SW = 250ηM. Error bars indicate mean ± standard error of triplicate samples. *D*, Cells were analyzed by FACS for CTLA-4 and CD28 staining and data is shown as a ratio of CTLA-4/CD28 MFI. The results are representative of three independent experiments. Error bars indicate mean ± standard error of triplicate samples. *E*, Cells were

analyzed by FACS for CFSE staining as indicated after 3 days in culture. Numbers above peaks indicate percentage of total. Shown are gated on $CD4^+$ cells. The results are representative of five independent experiments.

Fig. 6. Regulation of autoimmunity by the hexosamine pathway. *A-C*, Splenocytes were isolated from wild-type mice 11 days after immunization with MBP+CFA and re-stimulated *in vitro* with MBP for 4 days in the presence (green) or absence (red) of GlcNAc (40mM). *A*, Cells were stained with L-PHA-FITC and LEA-FITC (a lectin specific for poly-N-acetyllactosamine) and analyzed by FACS. Black line represents autofluorescence. *B*, Harvested supernatant were analyzed by ELISA for IFNγ and IL-6 production. . Error bars indicate mean ± standard error of duplicate samples and P values determined by Student t test. IL-4 was below ~30 pg/ml, the detection limit of our ELISA. *C*, 3.6 million $CD3^+$ T cells were injected into naïve $Mgat5^{+/-}$ mice (n=7 for each condition) and scored for signs of EAE daily for 30 days. *D,* The drinking water of female NOD mice was supplemented with (n=15) or without (n=15) 250μg/ml GlcNAc starting between 5-6 weeks of age. Mice were assessed for glycosuria weekly, with diagnosis of diabetes made after two consecutive positive tests of ≥2000 mg/dl glucose by Chemstrip 1 week apart. P values for EAE and diabetes incidence was determined by Fisher's exact test. P values for EAE mean score, disease duration and highest clinical score were determined by the Mann-Whitney test.

Fig. 7. A model for environmental and genetic regulation of autoimmunity via GlcNAc-branched N-glycans.

Supplemental Fig. 1. Metabolic regulation of β1,6GlcNAc-branched N-glycan expression in Jurkat T-cells by the hexosamine pathway**.** *A-C*, The indicated monosaccharides and metabolites were cultured with Jurkat T-cells for 3 days, stained with L-PHA or LEA (a lectin specific for poly-N-acetyllactosamine) and analyzed by FACS. Green, blue and red lines refer to altered glucose concentration in the culture media as indicated; all others were grown in 10 mM glucose. Error bars indicate mean ± standard error of triplicate staining.

Supplemental Fig. 2. Metabolic regulation of β1,6GlcNAc-branched N-glycan expression in primary mouse T-cells by the hexosamine pathway. *A*, Splenocytes from wild-type mice orally supplemented with (n=2) or without (n=2) GlcNAc for 5 days via their drinking water at the indicated concentration were stained with L-PHA-FITC in triplicate and analyzed by FACS. On average, mice drank ~4.6 ± 0.25 ml/day, estimated by determining the amount of GlcNAc solution remaining daily. For a 28.5g mouse, the approximate mg/kg dose received is 40. Error bars indicate mean ± standard error. P values were determined by the Mann Whitney t test. *B*, $CD3^+$ T-cells from wild-type mice stimulated with anti-CD3 antibody in the presence or absence of GlcNAc and/or swainsonine (SW) as indicated for 3 days were stained with L-PHA-FITC and analyzed by FACS. The results are representative of three independent experiments.

Supplemental Fig. 3. Metabolic regulation of T cell function by the hexosamine pathway. *A-F*, Wild-type splenocytes *(A-C,F)* and CFSE labeled $CD3^+$ T cells *(D,E)* were stimulated with anti-CD3 antibody in the presence or absence of GlcNAc, swainsonine (SW) and/or deoxymannojirimycin (DMN) as indicated. *A and B*, Cells were stained for CD69 and analyzed by FACS as indicated. Shown are gated on $CD4^+$ cells. Y axis shows percentage of the total CD4+ population. SW=250ηM, DMN=2mM. The results are representative of three independent experiments. Error bars indicate mean ± standard error of triplicate samples. *C*, Supernatant harvested after 3 days of culture were analyzed by ELISA for IFNγ. Data shown as percentage change from non-treated cells. The results are representative of three independent experiments. Error bars indicate mean ± standard error of triplicate samples. *D and E*, Cells were analyzed by FACS for CFSE staining as indicated after 3 days in culture. Shown are gated on $CD4^+$ cells. Numbers above peaks indicate percentage of total. The results are representative of three independent experiments. *F*, Cells were analyzed by FACS for 7-AAD staining. Shown are gated on

$CD4^+$ cells. Y axis shows percentage of the total $CD4^+$ population. SW= 250ηM, DMN=2mM. Error bars indicate mean ± standard error of triplicate samples.

Figure 1

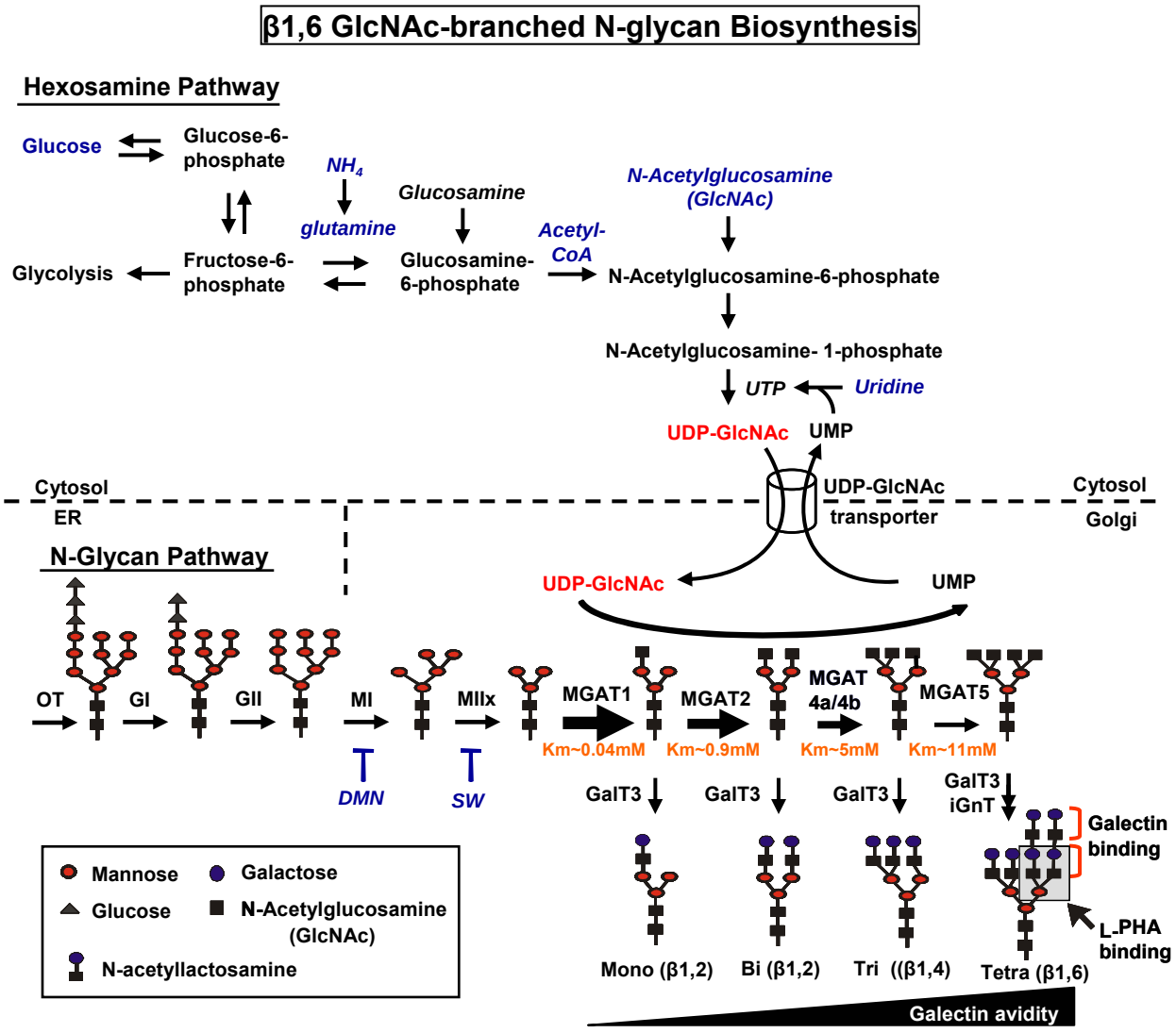

Figure 2

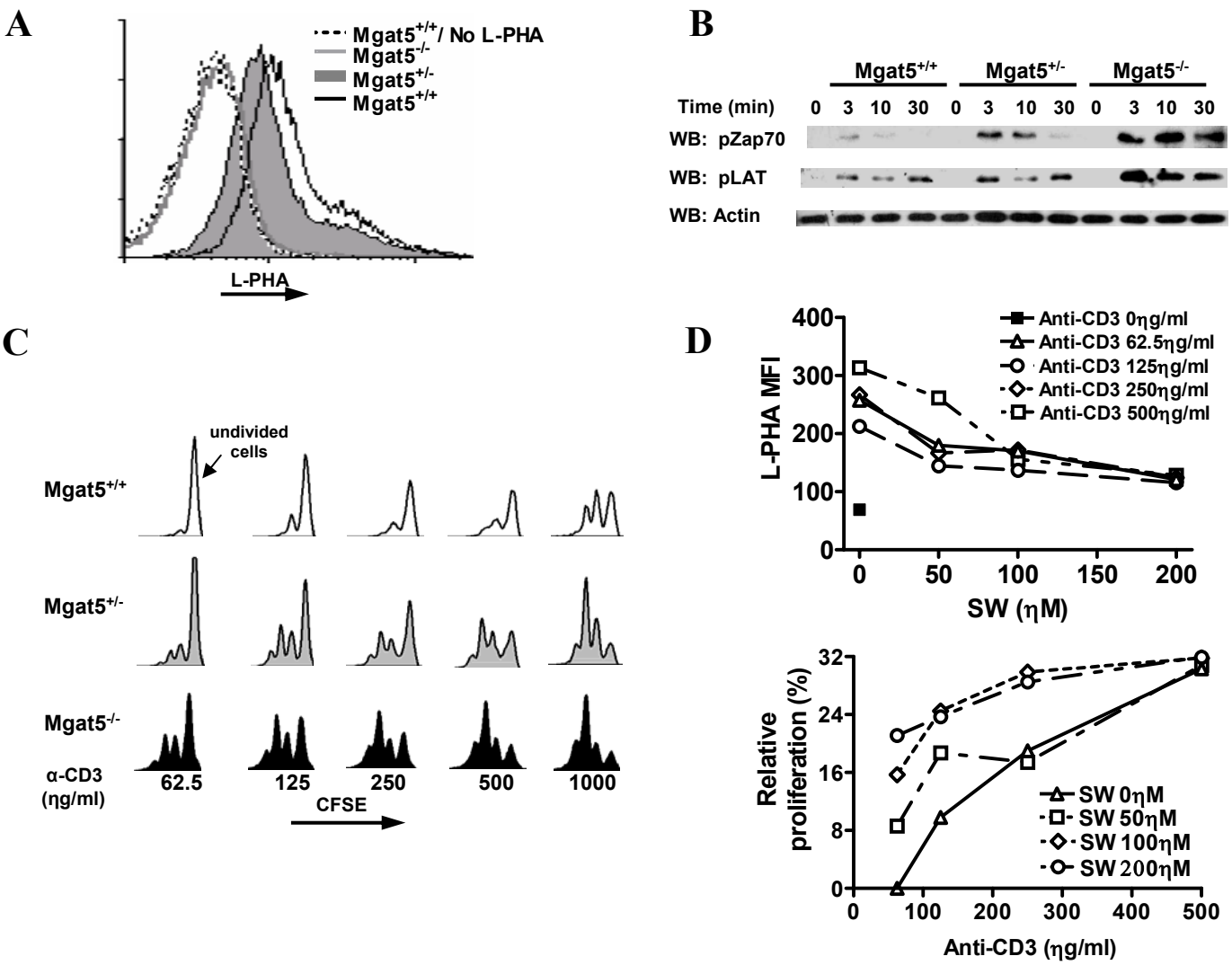

Figure 3

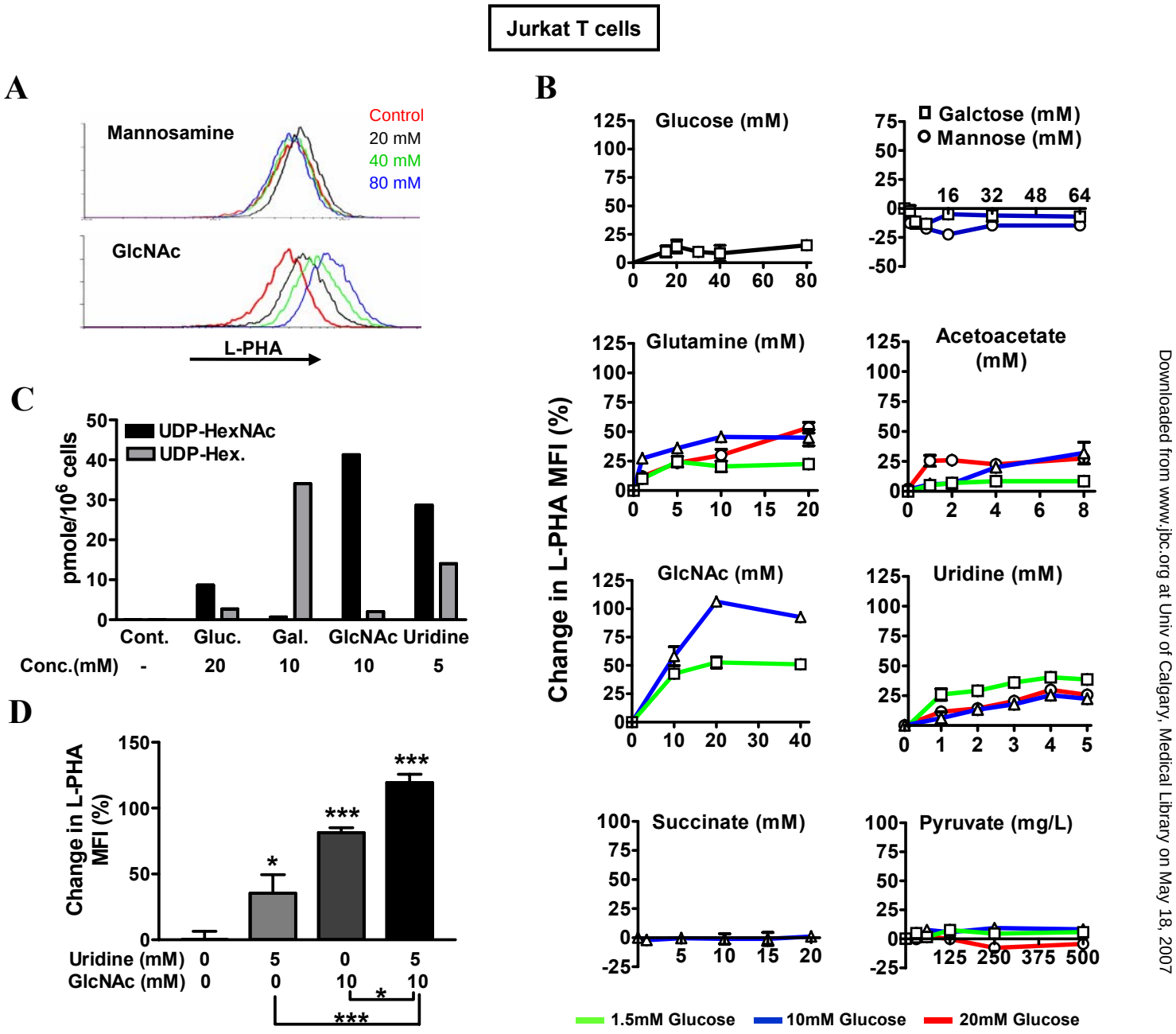

Figure 4

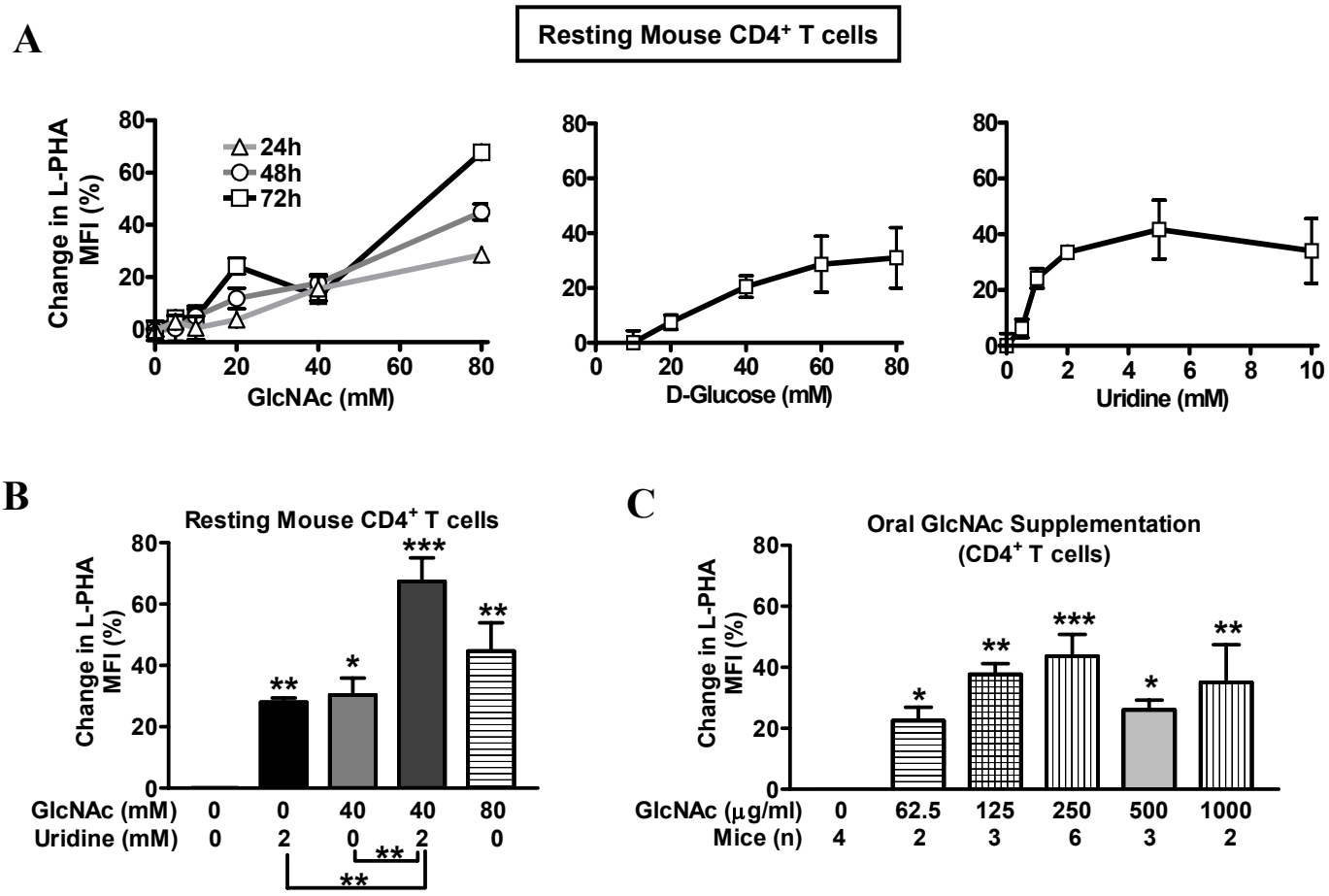

Figure 5

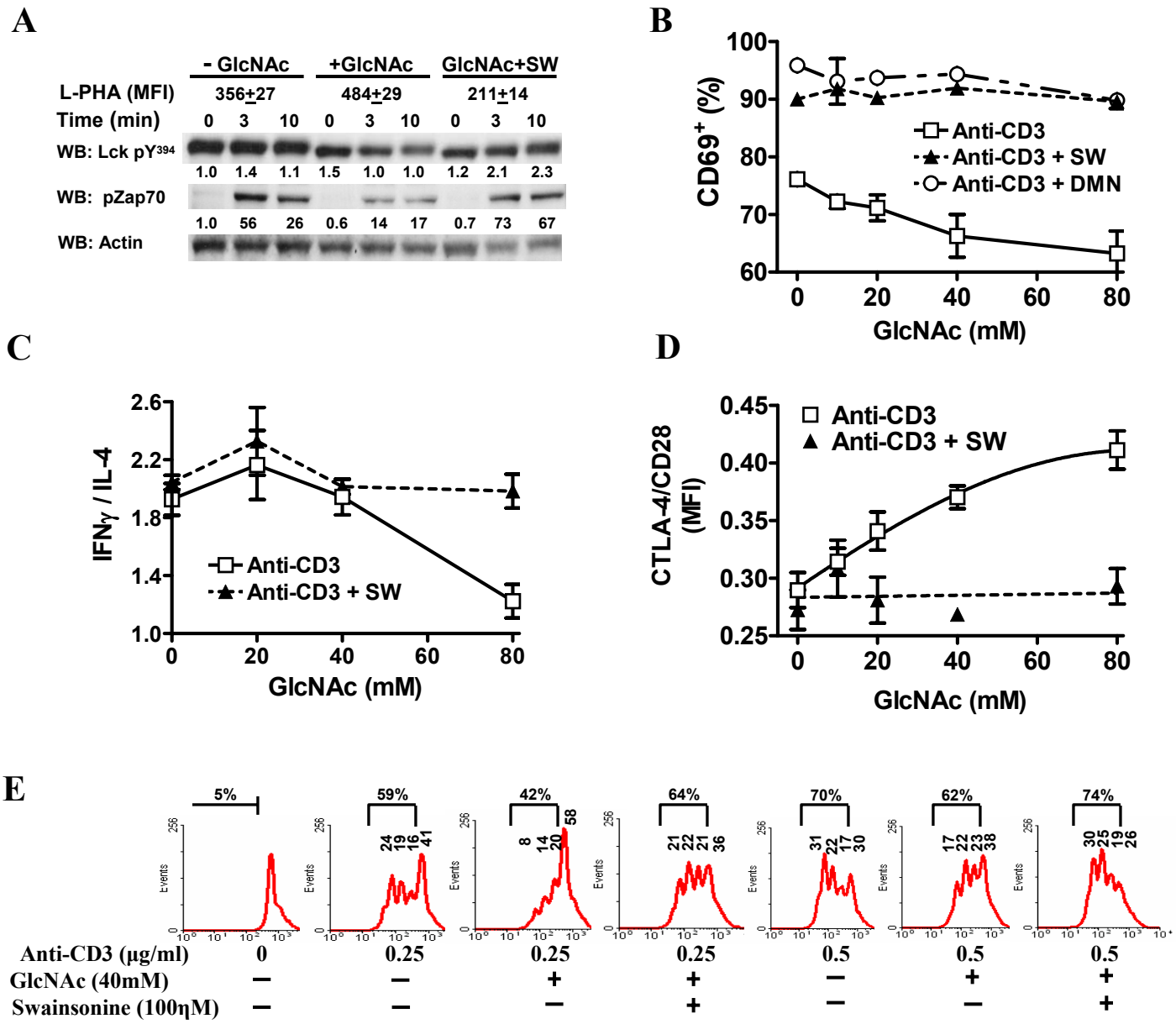

Figure 6

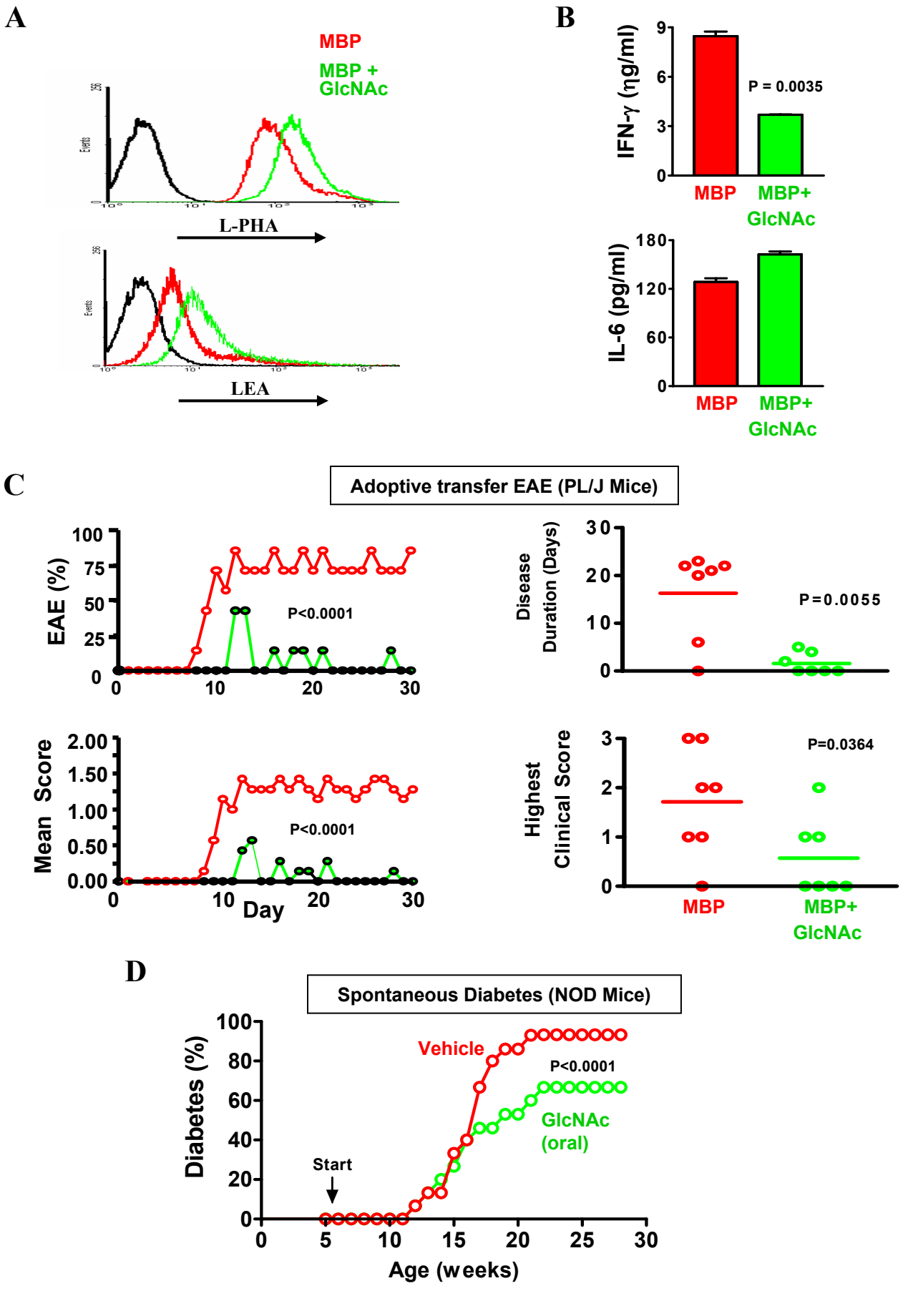

Figure 7

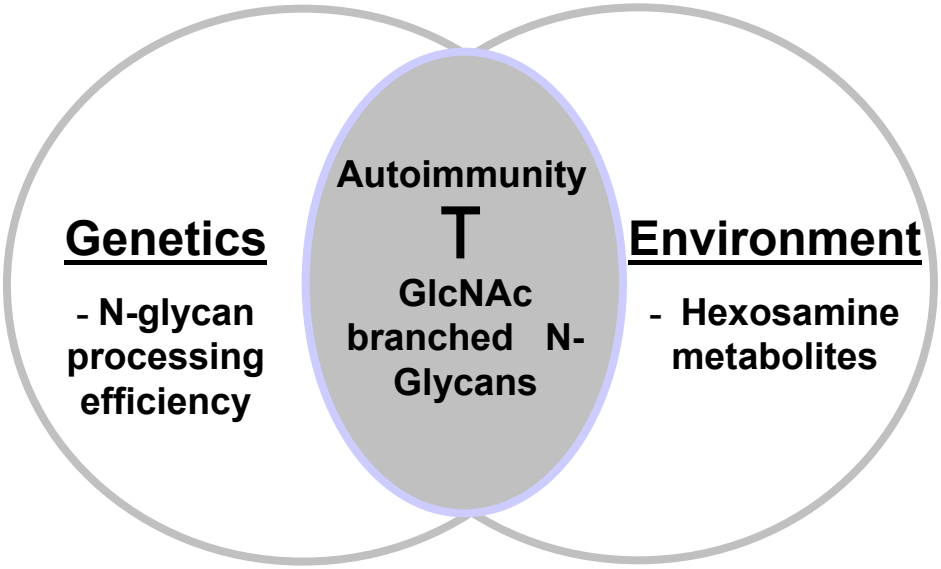

Supplemental Figure 1

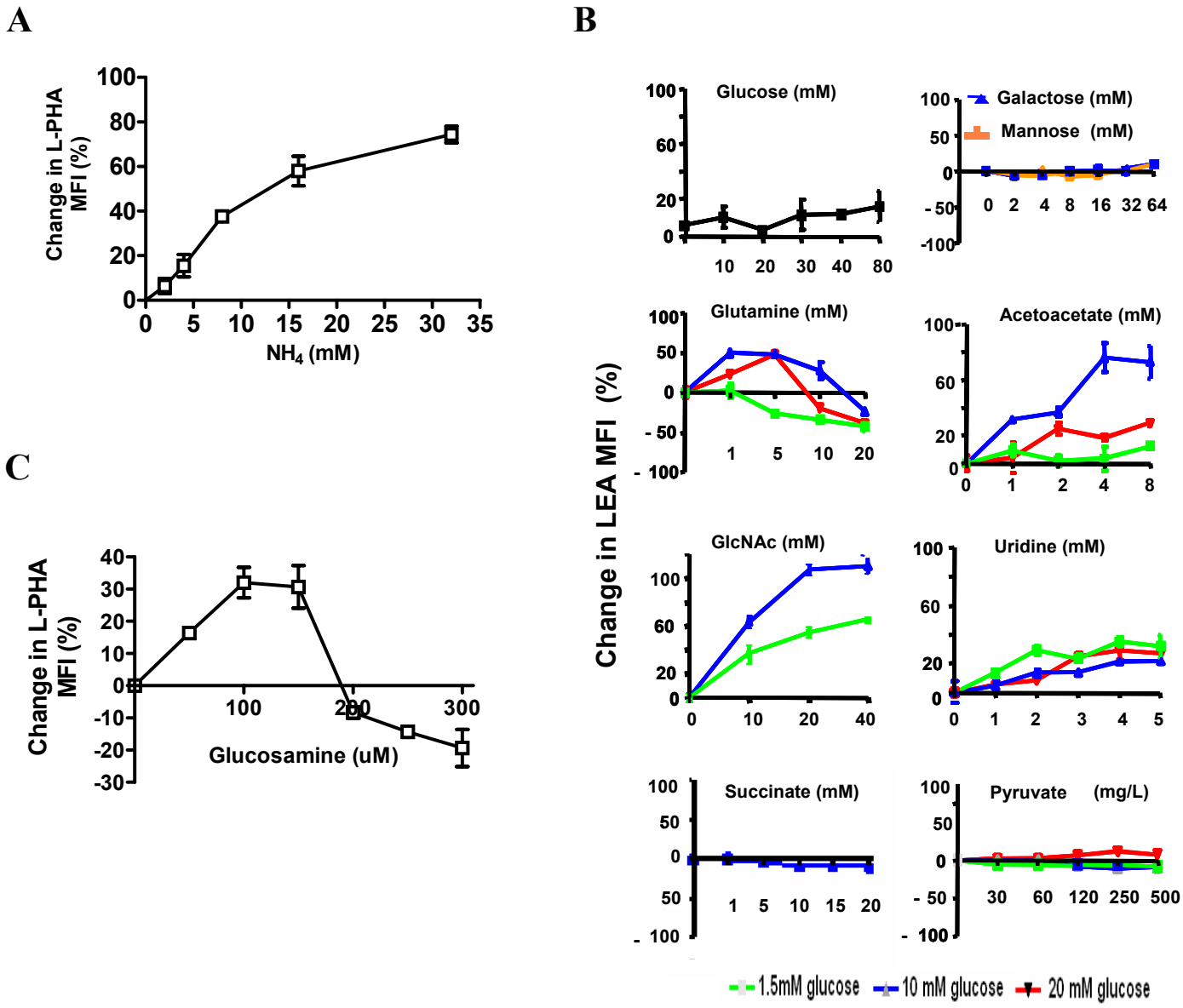

Supplemental Figure 2

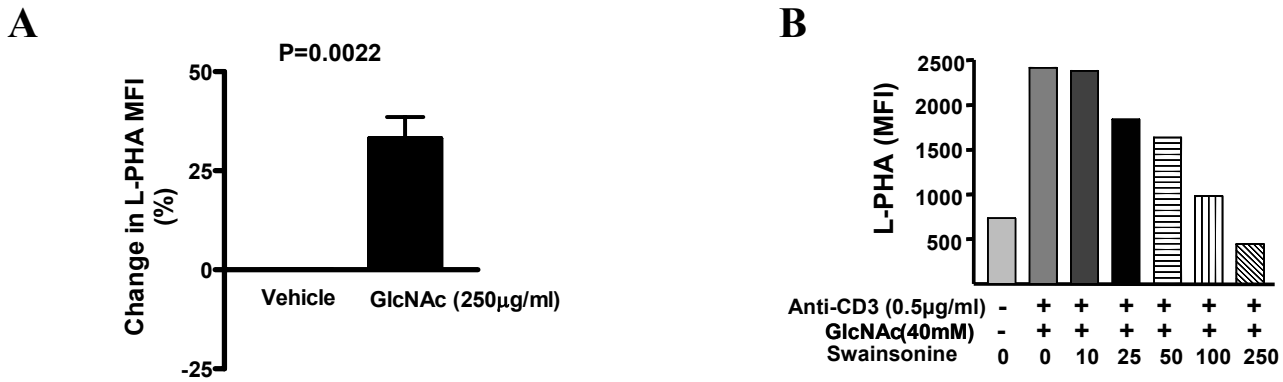

Supplemental Figure 3